Surface Morphology Studies of Multiblock and Starblock Copolymers of Poly(α-methylstyrene) and Poly(dimethylsiloxane)

Xin Chen and Joseph A. Gardella, Jr.*

Department of Chemistry, State University of New York at Buffalo, Buffalo, New York 14214

Philip L. Kumler

Department of Chemistry, State University of New York College at Fredonia, Fredonia, New York 14063

Received October 20, 1992; Revised Manuscript Received March 25, 1993

ABSTRACT: Surface morphology and compositions of multiblock and starblock copolymers of poly(α-methylstyrene) (PMS) and poly(dimethylsiloxane) (PDMS) were investigated by cross-sectional transmission electron microscopy, angle- and energy-dependent ESCA, and infrared spectroscopy. The extent of surface segregation of PDMS was determined for multiblock and starblock copolymers to a depth of 210 Å. No surface excess was detected at depths probed by attenuated total reflectance Fourier transform infrared spectroscopy measurements. The PMS–PDMS block copolymers with high PDMS bulk concentrations (60 wt %) have a highly oriented lamellar morphology in the near air surface region, and the topmost air surface region (27 Å) is exclusively composed of PDMS. The PMS–PDMS block copolymers with lower PDMS bulk concentrations (40 wt %) have lesser or no domain orientation and the surface region includes detectable PMS.

I. Introduction

The surface composition and morphology of block copolymers have been extensively studied in recent years both theoretically[1-3] and experimentally.[4-8] However, diblock and triblock copolymers were used in most of the previous surface investigations. There is little known about the surface morphology and composition depth profile of multiblock copolymers and, especially, of starblock copolymers.

Generally, phase separation behavior and surface segregation of binary component polymers have a direct relation to their structures. For example, in a binary homopolymer blend with interaction parameter χ and N repeat units of each homopolymer, phase separation begins at a critical polymer chain length N_c, which is given by the equation $(\chi N)_c = 2$ according to the Flory–Huggins theory.[9] For a symmetric AB diblock copolymer with N repeat units, a higher critical polymer block length N_c is given by the equation $(\chi N)_c = 10.5$, which was first derived by Leibler[10] from a mean field theory. For $(AB)_n$ starblock copolymers in which there are n arms and each arm is composed of a symmetric diblock with N repeat units, de la Cruz[11] predicted that $(\chi N)_c$ equals 8.86, 7.07, 5.32, and 4.33 for $n = 2, 4, 10$, and 30. When $n = 2$, an $(AB)_n$ starblock copolymer is an ABA triblock copolymer with the B block length twice as long as an A block length.

There have been few experimental studies of the surface morphology of multiblock copolymers and starblock copolymers in the literature (except polyurethane type multiblock copolymers).[12,13] In this paper, we present the poly(dimethylsiloxane) concentrations in the surface region of the multiblock and starblock copolymers of poly(α-methylstyrene) (PMS) and poly(dimethylsiloxane) (PDMS). The extent of surface segregation of the PDMS component, as measured by X-ray photoelectron spectroscopy (XPS or ESCA), is discussed as a function of bulk composition and block architecture. By use of the attenuated total reflectance FTIR (or ATR-FTIR) technique, a much thicker surface region of the block copolymers was studied. DSC experiments were carried out for the determination of the annealing temperature of the PMS–PDMS block copolymers. Transmission electron microscopy (TEM) results are included to show the relationship between the sampling depths of the surface-sensitive techniques and the morphological features of the block copolymers (i.e. domain size, shape, and orientation).

Table I. PMS–PDMS Block Copolymers

sample[a]	wt % PDMS	M_{PMS}	config-uration	total $M_w \times 10^{-5}$
1	40	8000	$(AB)_n$	1.31
2	60	8000	$(AB)_n$	1.19
3	70	8000	$(AB)_n$	2.55
4	45	9000	$(AB)_4C$	0.74
4	62	9000	$(AB)_4C$	0.97

[a] Samples 1–3 are multiblock copolymers. Samples 4 and 5 are four-arm starblock copolymers with poly(dimethylsiloxane) as the core block in each arm. A represents PMS block and B represents PDMS block. M_{PMS} is the weight average molecular weight of PMS blocks.

II. Experimental Section

Sample Preparation. Poly(α-methylstyrene), M_n of 80 000, was purchased from Aldrich Chemical Co. Poly(dimethylsiloxane) was purchased from Scientific Polymer Products. The PDMS was secondary standard with M_w of 1 010 000 and M_n of 180 000. PMS–PDMS multiblock and four-arm starblock copolymers were provided by Dr. Raymond F. Boyer of Michigan Molecular Institute; their structural information is shown in Table I. All polymers were used as received. Samples 1–3 are PMS–PDMS multiblock copolymers and samples 4 and 5 are four-arm starblock copolymers. The starblock copolymers have four arms and each arm is composed of a PDMS block (inner or core block) and a PMS block (outer block). To prepare the four-arm PMS–PDMS starblock copolymers, the PMS–PDMS diblock copolymers (the arm blocks) with active PDMS block ends were first synthesized and then linked to small molecules with four active sites at a controlled ratio. The molecular weights of polymers and polymer blocks given in Table I were measured by HPLC.

Polymer films (about 100 μm thick) for ESCA and ATR-FTIR measurements were cast from 1% chloroform solutions in clean Al weighing pans. The films were allowed to air-dry overnight, annealed at 140 °C for 3 days in a vacuum oven, and then analyzed without any further preparation. Any residual solvent in the

0024-9297/93/2226-3778$04.00/0

polymer films would have been detected by the presence of a chlorine signal in the ESCA spectrum. No solvent could be detected in the films within the detection limits of ESCA (less than 1 atom %). For transmission (TX) FTIR experiments, block copolymer films were cast on thin KBr pellets which were freshly prepared by pressing dry KBr powders. The polymer–KBr mixtures were ground and then pressed into pellets again. The TX-FTIR and ATR–FTIR results were averaged from the measurements of at least three separately prepared samples to ensure reproducibility. The air side of the polymer films was measured by both ESCA and ATR-FTIR.

The microdomain structures of the PMS–PDMS block copolymers were examined by cross-sectional transmission electron microscopy. For this purpose, relatively thick (200–300 μm) PMS–PDMS block copolymer films were obtained by casting 2% polymer solutions in chloroform into glass petri dishes. The dry films in the glass petri dishes were annealed at 150 °C in a vacuum oven for 3 days. The petri dishes with films were immersed in triple distilled boiling water for 10 min. Then the films were peeled from the petri dishes. The films were dried again before ultrathin sectioning. The high electron density of PDMS, compared with PMS, led to sufficient contrast without the need for staining.

Instrumentation. The angle- and energy-dependent ESCA experiments were performed on a Perkin-Elmer Physical Electronics Model 5300 ESCA using a hemispherical analyzer. Both Mg $K\alpha_{1,2}$ and Ti $K\alpha_{1,2}$ X-rays were used as the excitation source. The source was operated at 300 W (15.0 kV and 20 mA). The base pressure was maintained at 10^{-8} Torr. Pass energies of 17.9 eV with Mg $K\alpha$ X-rays and 71.55 eV with Ti $K\alpha$ X-rays were employed for all high-resolution angle-dependent acquisitions. Three take-off angles of 15°, 45°, and 90° were used with Mg $K\alpha$ X-rays as excitation source. Only a 90° take-off angle was used when Ti $K\alpha$ X-rays were employed. Care was taken to check X-ray radiation damage on the polymer sample surface. During exposure times twice as long as that required for the ESCA analysis used, the atomic ratios of carbon, silicon, and oxygen of several selected PMS–PDMS block copolymer samples remained the same within the range of ESCA measurement error; this means that no significant radiation degradation could be detected. All data manipulation (peak area calculation, baseline subtraction, etc.) was accomplished using a Perkin-Elmer 7500 computer running PHI ESCA version 2.0 software.

Both TX-FTIR and ATR-FTIR experiments were performed on a Mattson Polaris FTIR spectrometer with a DTGS detector at a resolution of 4 cm^{-1}. For collections of TX-FTIR and ATR-FTIR spectra, 16 and 32 scans were run respectively. A Harrick parallelogram Ge prism (50 × 10 × 3 mm), mounted on a Harrick TPMRA attachment, with a 45° face cut was used as the internal reflectance element for all ATR-FTIR collections. The depth of penetration (d_p) in the polymer films for the ATR-FTIR experiments was estimated to be 0.8–1.0 μm,[14] which led to a sampling depth (d_s, which is defined as $d_s = 3d_p$) of 2.4–3.0 μm from the air surface for the IR absorption bands between 700 and 800 cm^{-1}.

The ultrathin cross sections of the films were sliced normal to the film surface at liquid nitrogen temperature using a Reichert-Jung Ultracut E ultratome with a cryosectioning attachment. A transverse cross section was microtomed parallel with the air surface to avoid stretching the materials in the surface region. The electron micrographs were taken on a JEOL 100CX-II transmission electron microscope operating at 80 kV.

A TA Instruments 2910/2000 differential scanning calorimeter (DSC) was used for the determination of the glass transition temperatures (T_g) of poly(α-methylstyrene) homopolymer and the PMS blocks of the PMS–PDMS block copolymers. All samples were dried (at 55 °C in a vacuum oven overnight) before being loaded in DSC. During the DSC measurement, the samples of PMS homopolymer and the PMS–PDMS block copolymers were heated from 25 to 300 °C at a rate of 20 °C/min with a continuous nitrogen flow at a rate of 20 cm^3/min. The samples were then quench cooled to 25 °C with liquid nitrogen and reheated to 300 °C at the same rate of the first heat. The T_g was taken as the onset of slope change in the thermogram of the second heat.

Table II. Domain Features of the PMS–PDMS Block Copolymers

	domain features		
sample	shape	orientation[a]	period (Å)[b]
1	short lamellae	no orientation	180
2	medium lamellae	less oriented, parallel to surface	200
3	long lamellae	highly oriented, parallel to surface	210
4	PDMS Rods in PMS Matrix	no orientation	130
5	long lamellae	highly oriented, parallel to surface	300

[a] Orientation of PDMS domains in the plane of the cross section of the TEM samples. [b] Distance measured from a domain to the next domain of the same kind. Average was taken from five to eight consecutive domains.

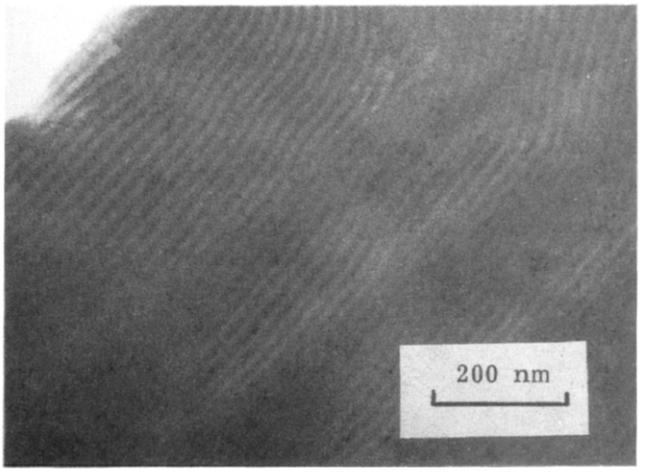

Figure 1. TEM micrograph of PMS–PDMS sample 3. The top left corner represent the air. Next to the air region is the surface region of the block copolymer. PDMS domains are the dark area.

III. Results

DSC Measurements and Annealing Temperature. Equilibrium morphological structures of multicomponent polymers can be approached by properly annealing as-cast samples. A multicomponent polymer has several T_g's, which correspond to its different components. The annealing temperature should be chosen well above the highest T_g of the multicomponent polymer. For PMS–PDMS block copolymers, there are two T_g's for PMS and PDMS blocks, respectively. The glass transition temperature of PMS determines the annealing temperature of the PMS–PDMS block copolymers. The T_g for both PMS homopolymer and PMS blocks in the PMS–PDMS block copolymers was measured to be 93 ± 2 °C, which is in good agreement with the T_g reported.[15] An annealing temperature of 150 °C for the PMS–PDMS block copolymers is appropriate. No thermal degradation up to 150 °C was detected.

TEM Measurements. The TEM micrographs of all of the five block copolymer samples were taken. Their morphological features are summarized in Table II. Figures 1 to 3 are representative TEM micrographs showing the morphology of the block copolymers in the near air surface region.

Some correlation between polymer chain structure and morphology can be made from the data in Table II. Samples 1 to 3 are PMS–PDMS multiblock copolymers with different bulk compositions, but the PMS blocks have the same length. For the sample with higher PDMS concentration, the PDMS block length is longer. The TEM

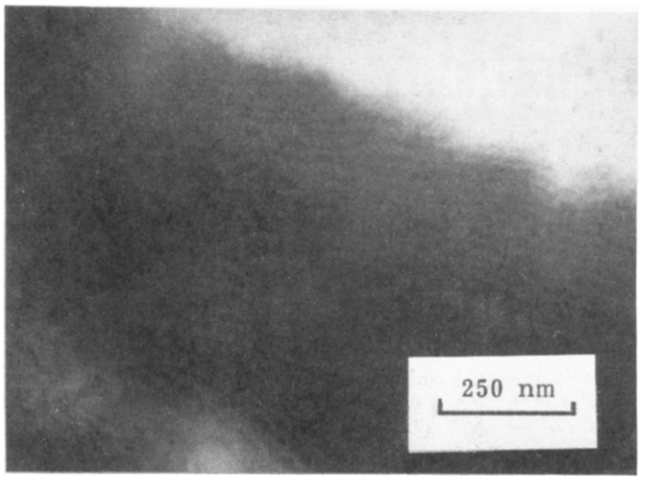

Figure 2. TEM micrograph of PMS–PDMS sample 2. The top right corner represent the air. Next to the air region is the surface region of the block copolymer.

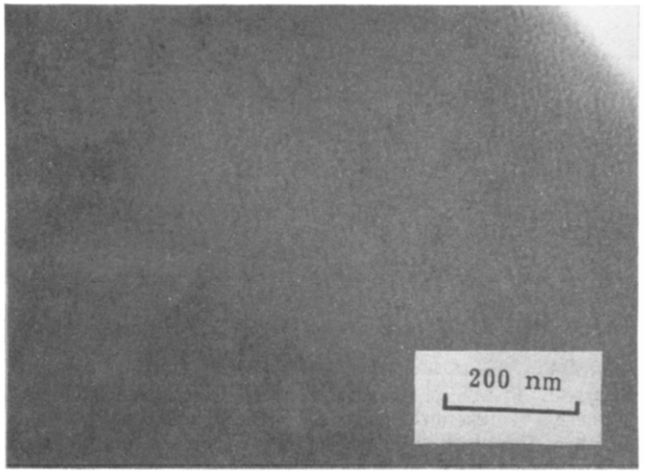

Figure 3. TEM micrograph of PMS–PDMS sample 4. The top right corner represent the air. Next to the air region is the surface region of the block copolymer.

results reveal that the multiblock copolymer sample with longer block length has a larger domain size. All three multiblock copolymer samples have lamellar morphology, but the length and the orientation of the lamellae vary from the bulk compositions. For the sample with longer PDMS blocks, the lamellae are longer and they are more likely oriented parallel to the air surface.

The starblock copolymers have the same trend as multiblock copolymers, but the morphology is more complicated. At lower PDMS bulk concentration (sample 4), the PDMS domains are not continuous in the cross-section plane. The PDMS domains most probably exist as rods with hexagonal packing in continuous PMS matrix. When the PDMS bulk concentration is high (sample 5), both PMS and PDMS domains are continuous and the lamellae orient parallel to the air surface.

No direct correlation of morphology between multiblock copolymers and starblock copolymers can be observed from TEM micrographs. Samples 1 and 4 have similar bulk composition, as do samples 2 and 5. Samples 2 and 5 have the same shape of domain, but the domain size and domain orientation are quite different. For samples 1 and 4, both domain shape and size are very different.

ESCA Measurements. Angle- and energy-dependent ESCA experiments were used to extract the surface compositions at different sampling depths.

ESCA Sampling Depths. The ESCA sampling depth depends on both take-off angle and the kinetic energy of emitted photoelectrons which are excited by the X-ray source. At a 90° take-off angle, the relationship between sampling depth (3λ) and kinetic energy of emitted photoelectrons is defined by an empirical equation[16]

$$\lambda\ (\text{Å}) = 490/E_k^{\,2} + 1.1E_k^{\,1/2} \qquad (1)$$

where E_k is the kinetic energy of the emitted photoelectron and λ is the inelastic mean free path of the emitted photoelectrons. The ESCA sampling depth (d_s) is generally defined as 3λ. Within 3λ of a polymer surface region, about 95% of the total emitted photoelectrons at a particular take-off angle are measured. The kinetic energy E_k of an emitted photoelectron from a certain atom is related to the binding energy of the atom (E_b) and the energy of the X-ray sources ($h\nu$), as described in the following equation.

$$E_k = h\nu - E_b \qquad (2)$$

The energy of the X-ray sources, $h\nu$, used in the current work is 1253.6 eV for Mg Kα X-rays and 4510.9 eV for Ti Kα X-rays. The ESCA sampling depths for C, O, and Si are listed in Table III.

Table III. ESCA Sampling Depths and X-ray Sources[a]

	binding energy (eV)	kinetic energy (eV)		sampling depth (Å)	
		Mg $K\alpha_{1,2}$	Ti $K\alpha_{1,2}$	Mg $K\alpha_{1,2}$	Ti $K\alpha_{1,2}$
C 1s	285.3	968.3	4225.6	102.7	214.5
O 1s	533.1	720.5	3977.8	86.5	207.3
Si 2p	102.7	1150.9	4408.2	112.0	219.1
Si 1s	1844[b]	c	2668.0	c	170.4

[a] The energies of Mg $K\alpha_{1,2}$ and Ti $K\alpha_{1,2}$ X-rays are 1253.6 and 4510.9 eV, respectively. [b] Estimated by the average of the two peaks at 1842.5 and 1845.5 eV in the ESCA high-resolution Si 1s window with Ti $K\alpha_{1,2}$ as X-rays. [c] The binding energy of Si 1s electrons is larger than the energy of Mg $K\alpha_{1,2}$ X-rays. There is no Si 1s electron emitted.

As of many other surface techniques, signal attenuation effect exists in the ESCA experiment. The emitted photoelectrons in the energy range of 50–1000 eV typically will travel only 20–100 Å before they lose energy from inelastic scattering events and cannot contribute to the photoelectron peak characteristic for a given element. At a particular take-off angle θ, about 65% of the total emitted photoelectrons originate within 1λ sin θ of the surface, 86% originate within 2λ sin θ, and approximately 95% originate within 3λ sin θ of the surface.[16-18] The emitted photoelectrons from different depths do not equally contribute to the ESCA signal measured. Therefore, the surface attenuation effect of signals should be considered when the ESCA data of different sampling depths are interpreted.

ESCA Calculations. Carbon to silicon atomic ratios were calculated from the measurements of carbon 1s (binding energy = 285 eV) peak areas and silicon 2p (binding energy = 103 eV) peak areas for data collected by using Mg X-rays. The sampling depths for C 1s and Si 2p are very close.

For Ti anode experiments, the Si 2p peak overlaps with an oxygen satellite peak arising from Ti Kβ X-ray radiation;[19] thus, the Si 2p peak was not used. Carbon 1s to oxygen 1s peak area ratios were chosen to calculate the surface compositions of the PMS–PDMS block copolymers, since the sampling depth for O 1s is closer to that of C 1s then the sampling depth for Si 1s (see Table III). ESCA signal from Si 1s photoelectrons originates from a significant shallower surface region than the signal from C 1s does.

Table IV. PDMS (wt %) at Surface of the PMS-PDMS Samples

sample	15° (27 Å)[a]	45° (73 Å)[a]	90° (103 Å)[a]	90° (214 Å)[b]	bulk
1	92.3 ± 1.7	68.4 ± 1.5	59.1 ● 1.2	57.5 ± 2.4	40
2	97.9 ± 0.8	85.2 ± 1.8	77.6 ± 2.2	70.4 ± 1.8	60
3	100 ● 1.0	87.0 ± 1.0	83.2 ± 1.1	82.8 ± 0.1	70
4	92.3 ± 1.6	67.0 ± 3.7	58.0 ± 3.1	59.2 ± 3.5	45
5	101 ● 0.7	85.2 ± 0.9	77.4 ± 1.4	73.0 ± 1.1	62

[a] ESCA take-off angles and sampling depths with Mg Kα as X-ray source. PDMS wt % was calculated from the Si 2p/C 1s ratios measured by ESCA. [b] ESCA take-off angle and sampling depth with Ti Kα as X-ray source. PDMS wt % was calculated from the O 1s/C 1s ratios measured by ESCA.

Based upon the structures of the repeat units of PMS (containing nine C atoms and no Si and O in each repeat unit) and PDMS (containing two C, one Si, and one O atoms in each repeat unit) segments, the DMS molar fraction is given by the equation

$$C/Si \text{ (or } C/O) = [2X + 9(1 - X)]/X \quad (3)$$

where C/Si (or C/O) is the atomic ratio of carbon to silicon (or oxygen) of the polymer film surface as measured by ESCA and X is the bulk DMS molar fraction of the samples.

PDMS weight percentage (W) of the PMS–PDMS block copolymers can be calculated from DMS molar fraction (X) according to the formula weights of the two repeat units.

$$W = 100 \times 74X/[74X + 118(1 - X)] \quad (4)$$

ESCA Measurements. Table IV lists the PDMS wt % of the surface region of PMS–PDMS block copolymers. A significant amount of excess of PDMS in the near surface region can be observed for all five samples, as expected from the much lower surface tension of PDMS relative to that of PMS. The PDMS concentration decreases as the ESCA sampling depth increases. Even when the sampling depth is over 200 Å (using the Ti anode), PDMS surface concentrations measured are still larger than their bulk concentrations.

From samples 1 to 3, the bulk PDMS concentrations increase from 40% to 70%. For the sample with the lowest PDMS bulk concentration (sample 1), the topmost layer (27 Å) of the multiblock copolymer does not consist exclusively of PDMS. This topmost layer is however composed of pure PDMS when the bulk PDMS concentration is at least 70%.

The surface compositions of the starblock copolymers (samples 4 and 5) exhibit a similar trend. The topmost 27-Å layer is completely composed of PDMS when the PDMS bulk concentration is at least 60%. The ESCA results are in very good agreement with the surface morphology revealed by the TEM micrographs. For the samples with no orientation parallel to the air surface (samples 1 and 4), the topmost surface region is not completely covered by PDMS. Some of the PMS lamellae, as of sample 1, expose their ends to the surface. The ends of those PMS lamellae in the near surface region can be measured by ESCA. For those samples with highly oriented lamellar domains in the surface region (samples 3 and 5), the topmost surface region fully consists of PDMS blocks, which have much lower surface energy than PMS blocks.

FTIR Measurements. Figure 4 shows TX-FTIR spectra of PMS and PDMS homopolymers and a PMS–PDMS block copolymer (sample 3) comprised of 70 wt % PDMS in the range of 650–1300 cm^{-1}. An ATR-FTIR spectrum of the PS-PDMS block copolymer (sample 3) is also shown in this figure. PMS has a very strong absorption peak at 700 cm^{-1} (out-of-plane bending of C–H bonds on benzene ring) while PDMS has a very strong absorption peak at 800 cm^{-1} (out-of-plane bending of C–H bonds on $-OSi(CH_3)_2-$ groups). These two peaks in the PMS–PDMS block copolymers are well separated but close enough to avoid a significant difference in the sampling depths, which are proportional to the wavelengths of the incident light. For IR quantitative measurements, both peak heights and peak areas were considered. Lab Calc/Square Tools were used to process the spectra. Six bands (863, 820, 800, 762, 700, 678 cm^{-1}) were picked to fit the IR absorbance from 940 to 670 cm^{-1}. The band at 800 cm^{-1} represents the contribution from PDMS and the band at 700 cm^{-1} represents the contribution from PMS. The ratios of the peak area of the curve-resolved component at 800 cm^{-1} to that at 700 cm^{-1} were calculated for all the five samples. The peak area ratio, A_{700}/A_{800}, can thus be used to indicate the relative amount of the two components in the PMS–PDMS block copolymers.

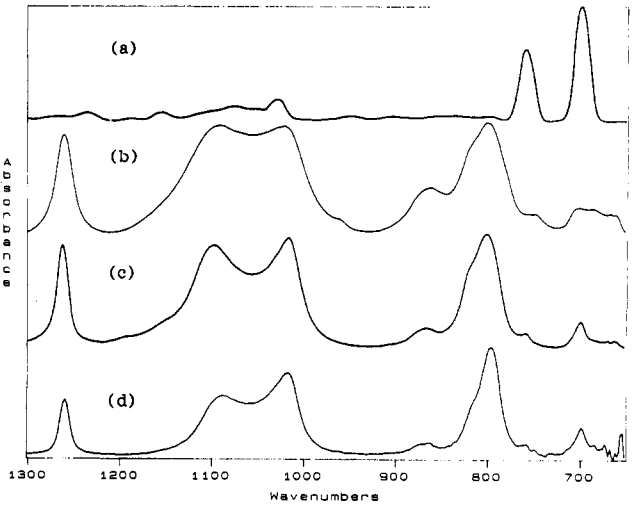

Figure 4. TX-FTIR spectra of PMS (a), PDMS (b), PMS–PDMS sample 3 (c), and ART-FTIR spectrum of PMS–PDMS sample 3 (d). Spectra c and d have the same peak ratio, A_{700}/A_{800}.

Table V. FTIR Results

sample	peak area ratio, A_{700}/A_{800} TX-FTIR	ATR-FTIR
1	0.29 ± 0.01	0.29 ● 0.03
2	0.17 ± 0.02	0.20 ± 0.03
3	0.11 ± 0.01	0.12 ± 0.01
4	0.23 ± 0.01	0.24 ± 0.02
5	0.15 ● 0.01	0.14 ± 0.01

PMS–PDMS block copolymer films were cast on KBr pellets. The pellets were crushed and ground and then pressed into pellets again. This procedure of preparing TX-FTIR samples were used to avoid any possible morphological orientation of the PMS–PDMS block copolymers. The peak area ratios, A_{700}/A_{800}, obtained from TX-FTIR measurements in this way, are assured to represent the real relative compositions of the block copolymer bulk. ATR-FTIR meausrements of the peak area ratios, A_{700}/A_{800}, give the relative compositions of the block copolymers in the near surface region.

Table V is the summary of the TX-FTIR and ATR-FTIR results. The peak area ratios, A_{700}/A_{800}, of TX-FTIR and ATR-FTIR for each PMS–PDMS sample are the same within experimental error. The surface compositions for all five block copolymers measured by ATR-

FTIR are the same as their bulk compositions. The PDMS surface segregation effect cannot be detected by ATR-FTIR for the PMS-PDMS multiblock and starblock copolymers. The PDMS surface segregation effect exists only in the surface region which is significantly less than the sampling depth of the ATR-FTIR measurements (2.4–3.0 μm) for those samples.

IV. Discussion

Morphological structures of block copolymers depend on such effects as block architecture, composition, segment–segment interaction parameter, and block length. The effect of block architecture on the surface of block copolymers has been intensively investigated in a previous study of one diblock and two triblock copolymers of polystyrene (PS) and poly(dimethylsiloxane).[8] The composition of the near surface region of these PS–PDMS block copolymers differs if the block architecture changes among the three type constitutions. This block architecture effect arises from the different folding of the block chains which constitute the first few layers in the near surface region. In the present study, however, no significant correlation between block architecture and the surface composition is observed from the multiblock constitution to the four-arm starblock (with PDMS as core block in each arm) constitution, as illustrated by the comparisons of the surface composition depth profiles between samples 1 and 4, and between samples 2 and 5. However, there are some differences in their domain structures as shown in the TEM results.

The PMS–PDMS samples with high PDMS bulk concentrations (60–70 wt %) have alternating lamellar structure. Since the surface energy of PDMS is much lower than that of PMS, the first lamella at the free surface side of those PMS–PDMS samples (3 and 5) should be PDMS rich, as revealed by the TEM and ESCA results, for a minimized overall free energy. The lamellar PDMS domains at the topmost surface are continuous in the two dimensions parallel to the surface. A thin layer of pure PDMS was detected in the very top surface region. The thickness of this pure PDMS thin layer measured by ESCA is about 27 Å, which is much smaller than the expected thickness (150 Å for sample 3 and 180 Å for sample 5) estimated from their periods of domains and bulk compositions. One reason contributing to the unexpected thin pure PDMS layer may be the irregular orientation of the surface lamellae in some areas of the surface.

A PDMS-rich surface region was also observed from the ESCA measurement of the PMS–PDMS samples with lower PDMS bulk compositions. However, PMS was detected even in the very top surface region. The surface enrichment of PDMS is, again, attributed to the low surface energy of the PDMS component in the PMS–PDMS polymers. The presence of PMS in the topmost surface region, however, originates from the intrinsic domain structure of the block copolymers. The morphological structure of sample 4, for example, is most probably in the type of PDMS rods in a PMS matrix. The PMS domains are continuous in all three dimensions while the PDMS component does not have continuously planar phases, as shown in Figure 3. There are two competing tendencies determining the composition in the near surface region. The first one is the reduction of the surface energy of the air surface of the PMS–PDMS polymers. The arrays of PDMS rodlike domains arrange parallel to the surface in the near surface region and a PDMS domain array appears in the topmost surface region. This results in a PDMS surface enrichment. Furthermore, the rodlike PDMS

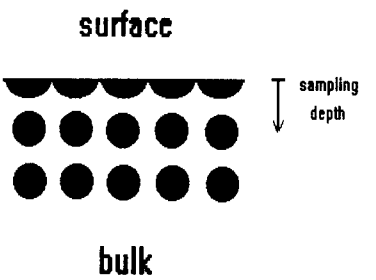

Figure 5. Schematic arrangement of the domains in the cross-section plane in the near surface region of the PMS–PDMS samples with the morphology of PDMS rods (black) in a PMS matrix.

domains in the topmost surface region become flattened to increase the coverage of PDMS on the surface, which minimizes the surface energy. On the the other hand, the tendency to reduce the interfacial energy between PMS domains and PDMS domains preserves the rodlike PDMS domains on the side in contact with PMS matrix. As a result of the two competing factors, an array of flattened rodlike PDMS domains is present in the topmost surface region and PMS constitutes the region between the PDMS domains for the PMS–PDMS samples with low PDMS bulk composition. A model shown in Figure 5 illustrates the arrangement of the domains in the plane of cross section in the near surface region of the PMS–PDMS samples with the morphology of PDMS rods in a PMS matrix.

V. Conclusion

Various techniques including ESCA, FTIR, TEM, and DSC were used to study PMS–PDMS multiblock and starblock copolymers. Angle- and energy-dependent ESCA and ATR-FTIR allowed these PMS–PDMS block copolymers to be studied at depths varying from the topmost 27 Å to a few micrometers.

A PDMS enrichment in the near surface region up to 200 Å was detected for all the multiblock and starblock copolymers with the bulk PDMS concentrations ranging from 40 to 70 wt %. For the PMS–PDMS block copolymers with high PDMS bulk concentration (60 wt % for starblock and 70 wt % for multiblock), the topmost 27-Å surface layer is exclusively composed of PDMS blocks and their domain structure is alternating PMS and PDMS lamellae. The domain structure for the PMS–PDMS block copolymers with low PDMS bulk concentration is characterized by either discontinuous PDMS domains or low order of PDMS domain orientation and the topmost surface region consists of PDMS blocks, as well as a very small amount of PMS blocks. ATR-FTIR measurements reveal that the PDMS segregation effect does not exist in the surface region sampled (up to 2–3 μm).

Acknowledgment. Financial support from National Science Foundation Polymers Program through Grant Number DMR8720650 is gratefully acknowledged. We also thank Drs. Terrence G. Vargo and Thaddeus M. Szczesny for their help.

References and Notes

(1) Fredrickson, G. H. *Macromolecules* **1987**, *20*, 2535.
(2) Shull, K. R. *Macromolecules* **1992**, *25*, 2122.
(3) Zielinski, J. M.; Spontak, R. J. *Macromolecules* **1992**, *25*, 589.
(4) Green, P. F.; Christensen, T. M.; Russell, T. P.; Jerome, R. *J. Chem. Phys.* **1990**, *92*, 1478.
(5) Shull, K. R.; Winey, K. I.; Thomas, E. L.; Kramer, E. J. *Macromolecules* **1991**, *24*, 2748.
(6) Hasegawa, H.; Hashimoto, T. *Macromolecules* **1985**, *18*, 589.

(7) Chen, X.; Gardella, J. A. *Polym. Prepr. (Am. Chem. Soc. Div. Polym. Chem.)* **1992**, *33* (2), 312.
(8) Chen, X.; Gardella, J. A., Jr.; Kumler, P. L. *Macromolecules* **1992**, *26*, 6621; *Macromolecules* **1992**, *26*, 6631.
(9) Flory, P. J. *Principles of Polymer Chemistry*; Cornell University Press: Ithaca, NY, 1953.
(10) Leibler, L. *Macromolecules* **1980**, *13*, 1602.
(11) Olvera de la Cruz, M.; Sanchez, I. C. *Macromolecules* **1986**, *19*, 2501.
(12) Graham, S. W.; Hercules, D. M. *J. Biomed. Mater. Res.* **1981**, *15*, 349.
(13) Graham, S. W.; Hercules, D. M. *J. Biomed. Mater. Res.* **1981**, *15*, 465.
(14) Harrick, N. J. *Internal Reflectance Spectroscopy*; John Wiley & Sons: New York, 1979; p 30.
(15) Gaur, U.; Wunderlich, B. *Macromolecules* **1980**, *13*, 1618.
(16) Seah, M. P.; Dench, W. A. *Surf. Interface Anal.* **1979**, *1* (1), 2.
(17) Payter, R. W. *Surf. Interface Anal.* **1981**, *3* (4), 186.
(18) Powell, C. J. *J. Electron Spectrosc. Relat. Phenom.* **1988**, *47*, 197.
(19) Vargo, T. G.; Gardella, J. A., Jr. *J. Vac. Sci. Technol.* **1989**, *A7* (3), 1733.